Available online at www.sciencedirect.com
ScienceDirect
International Journal of Pharmaceutics 324 (2006) 92–100
INTERNATIONAL JOURNAL OF PHARMACEUTICS
www.elsevier.com/locate/ijpharm

Pharmaceutical Nanotechnology

Nanoparticle encapsulation of emulsion droplets

Clive A. Prestidge *, Spomenka Simovic

Ian Wark Research Institute, University of South Australia, Mawson Lakes, SA 5095, Australia

Received 6 March 2006; received in revised form 15 June 2006; accepted 26 June 2006
Available online 5 July 2006

Abstract

The overall aim of this study is to coat emulsion droplets with nanoparticles using a simple heterocoagulation process in aqueous dispersion and determine: the adsorption behavior and interfacial layer microstructure, droplet physical stability against flocculation and coalescence, and the release profile of a model lipophilic molecule (dibutylphtalate (DBP)) from within the droplets. Polydimethylsiloxane (PDMS) droplets were used as a model emulsion due to their colloidal stability in the absence of added stabilisers. Aerosil™ type silica nanoparticles with different hydrophobicity levels were used as the model nanoparticles. The adsorption behavior of silica nanoparticles at the droplet–water interface was studied using adsorption isotherms and SEM imaging. Adsorption of hydrophilic nanoparticles is weakly influenced by pH, but significantly influenced by salt addition, whereas for hydrophobically modified nanoparticles a balance of hydrophobic and electrostatic forces controls adsorption over a wide range of pH and salt concentrations. The coalescence kinetics (determined under coagulation conditions at high salt concentration) and the physical structure of coalesced droplets were determined from optical microscopy. Adsorbed layers of hydrophilic nanoparticles introduced a barrier to coalescence of ~1 kT and form kinetically unstable droplet networks at high salt concentrations. The highly structured and rigid adsorbed layers significantly reduce coalescence kinetics. Significant sustained release of DBP can be achieved using rigid layers of hydrophobic silica nanoparticles at the interface. Activation energies for release are in the range 580–630 kJ mol^{-1}, 10 times higher than for barriers introduced by Pluronic® stabilisers.

Keywords: Emulsions; Nanoparticles; Encapsulation; Adsorption; Drug release

1. Introduction

Emulsions have been widely used as drug carriers in pharmacy as well as templates in the production of micro/nanocapsules and particles for controlled/targeted release and/or drug protection against environmental conditions (Courveur et al., 1995; Blanko-Prieto et al., 1998; O'Donnell and McGinity, 1997; Mehnert and Mader, 2001; Müller et al., 2000, 2002). Surfactant and/or polymer based emulsions are usually applied for these purposes. Particle stabilised emulsions are rarely used for pharmaceutical purposes, i.e. available data are scarce, even though it is well documented that particles can act as excellent emulsion stabilisers in both simple and multiple emulsions (Aveyard et al., 2003).

The first pharmaceutical emulsion vehicles based on particles were described by Oza and Frank (1989a,b). These authors reported the preparation, characterisation and release behavior of lidocaine in stable w/o/w multiple emulsions based on microcrystalline cellulose and conventional surfactants. Garti (1997a,b) suggested that particles could be particularly efficient in drug protection and controlled release due to a better sealed interface. Dry adsorbed emulsions (DAE) are specific emulsion carriers based on silica nanoparticles for controlled release of hydrophilic drugs (Rollet and Bardon, 2000; Chambin et al., 2000, 2002). Briefly, the first step of DAE preparation is to make a primary w/o emulsion by homogenising the oil phase and the drug-containing water phase. The second step is to blend the w/o emulsion with hydrophilic silica to produce a creamy liquid. The final step is to add hydrophobic silica to transform the liquid into a liquid powder with a particle size within the range from 100 to 1000 μm. DAE structure was investigated by scanning electron microscopy combined with chemical microanalysis and dying tests (Chambin et al., 2000) and by electron spin resonance (ESR) studies to follow the behavior of both liquid phases during the manufacturing process (Chambin et al., 2000). Each emulsion phase is adsorbed on silica adsorbents

* Corresponding author. Tel.: +61 8 83023569; fax: +61 8 83023683.
E-mail address: clive.prestidge@unisa.edu.au (C.A. Prestidge).

0378-5173/$ – see front matter © 2006 Elsevier B.V. All rights reserved.
doi:10.1016/j.ijpharm.2006.06.044

with a suitable polarity (silica) to obtain a free-flowing powder with nonporous particles of size from 125 to 710 μm, with small specific surface area and a spherical shape. DAE particles appear to be made up of a random pack of hydrophilic and hydrophobic particles, containing a liquid phase (aqueous and oily) adsorbed on silica of the same polarity by weak bonds. DAE have been formulated to be introduced into oral dosage forms such as tablets and hard gelatin capsules. A pharmaceutical application of DAE for the oral administration route has been made with chlorpheniramine maleate (Rollet and Bardon, 2000).

Emulsion stabilisation by solid particles depends largely on sufficient particle adsorption and the formation of a "densely packed" layer at the oil–water interface, which prevents droplet coalescence, i.e. the ability of particles to form rigid structures that can sterically inhibit droplet coalescence. If charged, particles can give rise to electrostatic repulsion, which facilitates emulsion stability against flocculation (Tambe and Sharma, 1994). The magnitude of the steric barrier is controlled by how difficult it is to remove the particles from the interface, which depends largely on the attachment energy that is a function of the contact angle (Tadros and Vincent, 1983; Tambe and Sharma, 1994; Binks and Lumsdon, 2000c). That is, the level of interparticle interaction determines the strength of the formed protective film (Tambe and Sharma, 1994). This situation implies that particle interactions at the droplet surface are dominated by attractive forces, which results in the formation of coherent monolayers with significant mechanical strength. Recent results have shown that stable emulsions can be formed even if the droplets are not completely covered by particles (Vignati et al., 2003; Binks et al., 2005; Horozov and Binks, 2006), which is not in accord with a steric stabilisation mechanism. Horozov and Binks (2006) have recently demonstrated the link between particle interactions in planar monolayers and the mechanisms of emulsion stabilisation. The authors showed that repulsive colloidal particles, which give well-ordered planar monolayers, can be effective emulsion stabilisers due to their spontaneous accumulation as a dense monolayer bridging emulsion droplets sparsely covered with particles and thus preventing coalescence. The significant particle density of the bridging monolayer is due to the strong capillary attraction between particles caused by the deformed menisci around them. Furthermore, at sufficiently high concentrations, colloid–laden interfaces exhibit viscoelastic behavior (Tambe and Sharma, 1993, 1994), which enhances emulsion stability by increasing the magnitude of steric hindrance and by retarding the rate of liquid drainage between coalescing droplets.

The effectiveness of particles in stabilising emulsions depends, therefore, on their particle size, wettability and initial location, as well as the level of interparticle interactions (Binks and Lumsdon, 1999, 2000a,b,c; Tambe and Sharma, 1994; Yan et al., 2001). The stabilising effectiveness is often rationalised in terms of the attachment energy, E (Binks and Lumsdon, 2000c) i.e. the energy to expel the particles from the interface into one of the bulk phases. For a spherical particle of radius R, at a planar oil–water interface of interfacial tension γ_{ow}, with θ the contact angle the particle makes at the interface (measured through the water phase), the attachment energy is:

$$E = \pi R^2 \gamma_{ow}(1 + \cos\theta)^2 \quad (1)$$

The sign within the bracket becomes negative for particle removal into the water phase. It follows that a particle is most strongly held at the interface for $\theta = 90^\circ$, is more easily removed into oil for $\theta > 90^\circ$ and more easily removed into water for $\theta < 90^\circ$.

In this work we highlight some fundamental aspects of particle stabilised emulsions connected to potential pharmaceutical applications. The core strategy is to coat emulsion droplets by nanoparticles using heterocoagulation processes under different solution conditions such as pH and ionic strength. Solution conditions can affect the interfacial nanoparticle layer structure, which in turn may affect the carrier properties, e.g. storage stability, drug release and *in vivo* fate. The potential advantages of nanoparticle coated emulsion droplets as drug carriers include: the cold and simple production procedure, the absence of organic solvents, enhanced drug protection and controlled drug release.

In this study we are concerned with nanoparticle encapsulated emulsions that possess significant potential as carriers for lipophilic molecules with enhanced stability, protection and controlled release properties in comparison with surfactant or polymer stabilised emulsions. Recently, we have reported the adsorption mechanisms and adsorbed layer structure for hydrophilic (Simovic and Prestidge, 2003a) and hydrophobic (Simovic and Prestidge, 2003b) nanoparticles at emulsion droplet–water interfaces. Moreover, the enhanced stability against coalescence for nanoparticle encapsulated emulsions has been demonstrated (Simovic and Prestidge, 2004; Prestidge et al., 2004). The current study explores the interplay between nanoparticle adsorption thermodynamics, adsorbed nanoparticle layer structure, droplet stability and the release behavior of a model lipophilic molecule from emulsion droplets encapsulated by nanoparticles of different hydrophobicities.

2. Materials and methods

2.1. Preparation and characterisation of nanoparticle coated droplets

The adsorption behavior of hydrophilic and hydrophobically modified silica nanoparticles of ~50 nm diameter at the polydimethylsiloxane (PDMS) droplet–water interface has been investigated through particle adsorption isotherms, with complementary studies of the adsorbed layer structure by freeze-fracture SEM. The influence of solution pH and electrolyte concentration has indicated the magnitude of particle–droplet and particle–particle interactions, and the influence of droplet cross-linking (deformability) has indicated the role of particle penetration through the droplet–water interface.

High-purity water (Milli-Q) was used throughout the study. Diethoxydimethylsilane (DEDMS) and triethoxymethylsilane (TEMS) were supplied by Aldrich (Milwaukee, WI) and redistilled under nitrogen prior to use. Ammonia (Aldrich), KNO_3, NaCl (Merck, Darmstadt, Germany) and other reagents used

Table 1
Properties of fumed silica nanoparticles

Trade name	Contact angle (°)[a]	BET surface area ($m^2\ g^{-1}$)	Average size (nm)[b]
Aerosil 380	14; 0	380 ± 30	7
Aerosil R816	23; 60	180 ± 20	12
Aerosil R711	55 ± 5; 67	130 ± 20	12
Aerosil R974	117 ± 4; 75	170 ± 20	12
Aerosil R812	118 ± 6; 86	260 ± 20	7

[a] Contact angles estimated from enthalpy of immersion (Yan et al., 2000); first (left) number: contact angle at water/air interface, second (right) number: contact angle at toluene/water interface.
[b] Refers to primary particles according to the manufacturer specifications.

were analytical grade. The nanoparticles used (Aerosils, supplied by Degussa) were fumed silica with various degrees of surface chemical modification and have water contact angles from 10° to 117° estimated from enthalpy of immersion data (Yan et al., 2000). These were dispersed in aqueous solution using an ultrasonic bath (300 W for 2 h). The most hydrophobic samples Aerosil R974 and R812 need to be dispersed using rotor–stator homogeniser prior to ultrasonic bath dispersing. Properties of the silica nanoparticles used are listed in Table 1. Dynamic light scattering confirmed effective dispersion and mean particle diameters of ∼50 nm for all nanoparticle samples investigated. Zeta potentials were determined using phase analysis light scattering (PALS) and were within the range −20 to −80 mV for PDMS droplets (0.1 wt.% at pH 9) and from −5 to −25 mV for silica nanoparticles (0.25 wt.% aqueous dispersions at pH 9) depending on the NaCl concentration (from 10^{-4} to 10^{-1} M NaCl). PDMS in water emulsions were prepared through the base catalyzed polymerisation of DEDMS using a modified method of that reported by Obey and Vincent (1994) and Goller et al. (1997). Aqueous solutions containing 1% DEDMS and 10% ammonia were sealed in a 250 ml reaction vessel, shaken vigorously for 30 s, and then tumbled at 30 rpm and 25 °C for 18 h. These were dialysed against water to purify. These droplets are composed of low molecular weight cyclic and linear PDMS, having a viscosity of ∼10 mN s m^{-2} and are termed "liquid". A further batch of cross-linked PDMS droplets were prepared using a 1:1 mixture of DEDMS and TEMS as the monomer and have been shown to be substantially viscoelastic. Drop size distributions were characterised by laser diffraction (Malvern Mastersizer X). Average drop sizes and size span [defined as $(d(v,0.9) - d(v,0.1))/d(v,0.5)$] are 1.25 μm and 0.56 for the liquid droplets, and 1.05 μm and 1.2 for the cross-linked droplets. Electrophoretic mobilities and hence ζ potentials were determined using either microelectrophoresis (Rank Bros, Mark H) or PALS.

Nanoparticle coating efficiency was determined from adsorption isotherms. Known volumes and concentrations of aqueous silica sols and PDMS droplets (of known interfacial area) were combined under mixing in reaction vials. The vials were sealed and equilibrated by tumbling at 30 rpm for 18 h at 22 °C. Upon attaining adsorption equilibrium, aliquots were removed, filtered through a hydrophilic membrane filter (MF-Millipore with pore size 0.45 μm) and analysed spectrophotometrically at λ = 250 nm for silica nanoparticle concentrations. We have shown that this filtration method removes PDMS droplets, but not the silica nanoparticles and allows adsorbed amounts to be determined by a depletion method. Silica nanoparticle adsorbed amounts (determined in triplicate) were calculated from the ratio of the adsorbed concentration and the PDMS droplet interfacial area. Errors in the adsorbed amount values were less than ±10%. Droplets with adsorbed nanoparticle layers were imaged using freeze-fracture scanning electron microscopy (Philips XL 30 FEG SEM with Oxford CT 1500 cryotransfer system). The methodology consisted of cryofixation, fracturing, etching, platinum coating and imaging (Hunter, 1993; Sawyer and Grubb, 1987; Robbe-Tomine and Hen-Ferrenbach, 1998). A freeze-fracture SEM method for studying particle arrangement at the surface of o/w and w/o emulsion droplets was reported by Binks and Kirkland (2002).

2.2. Droplet stability

The coalescence stability of PDMS emulsion droplets in the presence of silica nanoparticles has been investigated. The coalescence kinetics (determined under coagulation conditions at high salt concentration) and the physical structure of coalesced droplets were determined from optical microscopy. Droplet coalescence kinetics and the influence of various adsorbed nanoparticle layers was determined in the presence of salt (above the critical coagulation concentration (ccc) to screen the electrostatic interactions) by optical microscopic imaging (Olympus BH2, Sony low-light CCD camera and Optimas image analysis system). It is noted that though laser diffraction may give more statistically significant droplet size data, it cannot distinguish the flocculation and coalescence of emulsion droplets. Our aim here was to differentiate coagulated and coalescenced droplets; further details of the experimental protocol are given elsewhere (Simovic and Prestidge, 2004).

2.3. Release of dibutylphtalate

Dibutylphthalate (DBP) was chosen as a model poorly soluble drug (its solubility is ∼1 mg/100 ml in water at 20 °C) because it is a liquid and readily miscible with PDMS (as confirmed experimentally). Release profiles were determined from both uncoated and coated droplets so that the role of the nanoparticle stabilising layers can be specifically assessed. PDMS emulsion droplets containing DBP were prepared using the same method as described above and where the monomer (i.e. DEDMS) is pre-mixed with DBP (at up to 2.5%). The emulsion droplet size, size distributions and ζ potentials were not significantly altered by the presence of DBP. Partition coefficients (P = concentration of DBP in the PDMS droplets/concentration of DBP in the aqueous phase of the emulsion) of DBP in emulsions were determined by ultracentrifugation at 10 000 rpm for 30 min and subsequent HPLC analysis. $\log P$ was determined to be 3.18 ± 0.2. The partition coefficient is lower for a droplet/water system than for a planar oil/water system, because of increased interfacial area for drug partitioning.

Uncoated and nanoparticle coated droplet samples were prepared by mixing 10 ml of 1% PDMS emulsion with 10 ml of either MilliQ water or 10 ml of 1 wt.% silica aqueous dispersions, respectively. Salt concentrations were adjusted in the range 10^{-4} to 10^{-1} M NaCl in order to control the nanoparticle layer structure. After tumbling for 18 h at 30 rpm, samples were investigated further for drug dissolution profiles. Droplets were completely coated by silica nanoparticles in accord with previously reported isotherms. It should be noted that within the experimental error log *P* was unaltered upon droplet coating.

The performance of well-characterized interfacially adsorbed nanoparticle layers in controlling the oil-to-water transport kinetics of DBP has been determined using standard release kinetics methods, i.e. release profiles of DBP were determined using the USP rotation paddle method. Sampled aliquots (3 ml) from the dissolution medium (900 ml MilliQ water) were ultracentrifuged to separate the colloid carrier from the dissolved drug, which was subsequently analysed by HPLC (655A-11 Liquid Chromatograph (Shimadzu)) with a Platinum® EPS C18, 5 μm, reversed-phase column (Alltech), equipped with a UV detector. The detected limit was 10^{-6} g/100 ml. Considering that 10 ml of emulsion sample (containing 0.025 wt.% DBP) is dispersed in 900 ml of dissolution media, the maximum concentration of DBP in solution is therefore 0.28 mg/100 ml, which is significantly less than equilibrium solubility in water and hence sink conditions are fulfilled (Robinson and Lee, 1978).

3. Results and discussion

3.1. Preparation and characterisation of nanoparticle coated droplets

Adsorption isotherms for hydrophilic and hydrophobic silica nanoparticles (20–50 nm in diameter) adsorbed at PDMS droplets are given in Figs. 1 and 2, respectively. Silica nanoparticle–PDMS droplet interaction may be regarded as a heterocoagulation process between spherical colloidal particles of different radii and unequal surface potentials; thus it can be rationalised in terms of particle–droplet and particle–particle lateral forces. Particle–droplet interactions may be described by the extended DLVO theory of Hogg, Healy and Fuerstenau

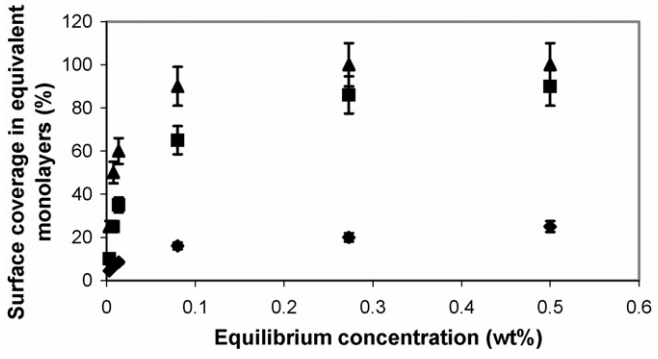

Fig. 1. Adsorption isotherms for hydrophilic silica (Aerosil R974) and PDMS droplets as a function of salt concentration (pH 9): (♦) 10^{-3} M NaCl; (■) 10^{-2} M NaCl; (▲) 10^{-1} M NaCl.

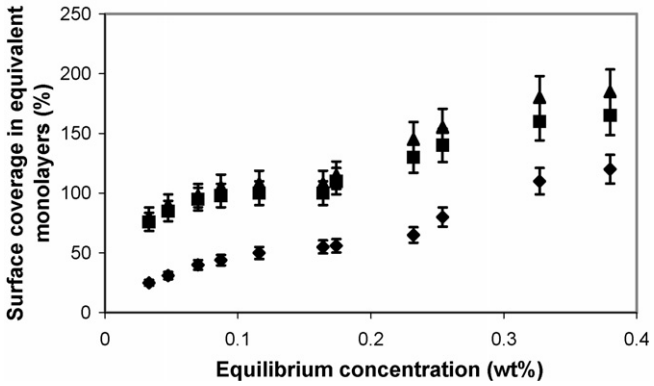

Fig. 2. Adsorption isotherms for hydrophobic silica (Aerosil R974) and PDMS droplets at pH 9 and in the presence of: (♦) 10^{-4} M NaCl; (■) 10^{-3} M NaCl; (▲) 10^{-2} M NaCl.

(HHF) (1966). The HHF model is restricted to binary systems in which the two components are of similar chemical type and with common potential determining ions, and is applicable to surface potentials less than 60 mV, when the double layer thickness is small in comparison with particle size and for large separation distances. The HHF model has been successfully used for solving numerous particle deposition problems (Adamzcik, 1989; Adamzcyk and Weronski, 1999; Bleier and Matijevic, 1997) e.g. adsorption of ludox silica onto PVC latex particles (Bleier and Matijevic, 1997). Using the HHF model an energy barrier for heterocoagulation of 3–5 kT was calculated under dilute salt conditions (10^{-4} to 10^{-3} M NaCl) hence indicating that particle–droplet normal interaction is not critical for adsorption and coating.

Adsorption was found to be determined by lateral particle–particle forces. More precisely, hydrophilic silica nanoparticles adsorb onto PDMS droplets with "Langmuirian isotherms" (Fig. 1) and plateau surface coverage values correspond to their effective particle size (hard sphere radius + double layer thickness) i.e. lateral silica–silica interaction controls particle packing**.** Based on the assumption that nanoparticles are adsorbed at the interface in a close packed monolayer, it can be shown that an adsorbed amount of ∼200 mg m^{-2} corresponds to monolayer coverage (Simovic and Prestidge, 2003a,b).

The free energy of adsorption (ΔG_{ads}) is in the range −15 to −23 kJ mol^{-1} and concordant with a physical adsorption mechanism, i.e. dispersion forces and hydrogen bonding are sufficient to overcome the electrostatic repulsion between nanoparticles and droplets. ΔG_{ads} and particle packing at the interface are only weakly influenced by pH, but significantly increased by salt addition. Droplet cross-linking reduced particle adsorption, but only at higher salt concentrations; this was attributed to the increased likelihood of silica nanoparticles wetting the PDMS and therefore interfacial penetration. Freeze-fracture SEM revealed that in the low salt regime (<10^{-2} M NaCl) individual silica nanoparticles are adsorbed at the droplet interface with negligible interfacial aggregation. Densely packed adsorbed particle layers are only observed when the double layer thickness is reduced to 1–3 nm nanometers, i.e. ≥10^{-1} M NaCl (Fig. 3).

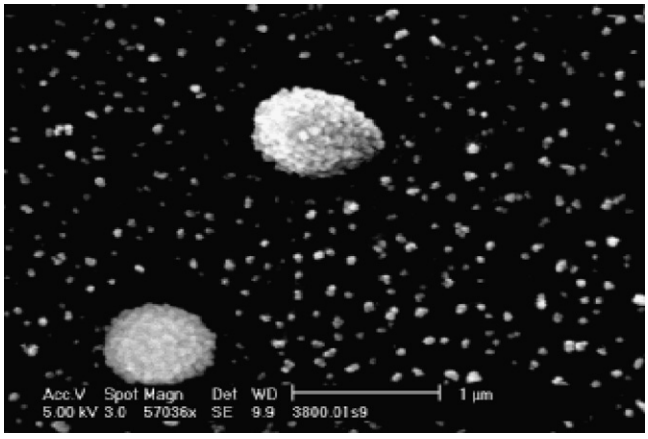

Fig. 3. Freeze-fracture SEM image of PDMS droplets coated by hydrophilic silica nanoparticles (pH 9; 10^{-2} M NaCl).

For hydrophobic silica nanoparticles surface coverage values increase to multiple layer values (Fig. 2) and interfacial particle saturation occurred at a salt concentration two orders of magnitude less than the critical coagulation concentration (ccc) for silica nanoparticles in water. The adsorption behavior and interfacial properties of hydrophobically modified silica nanoparticles are thus highly contrasting to those of hydrophilic nanoparticles. Firstly, adsorption isotherms for hydrophobically modified silica nanoparticles (θ in range 30–117°) are of significantly higher affinity than for hydrophilic nanoparticles, show evidence of multi-layer coverages (non-Langmuirian adsorption) and are strongly dependent on droplet cross-linking, i.e. interfacial penetration. That is, for liquid PDMS droplets adsorption isotherms are sigmoidal (Fig. 2), whereas for cross-linked PDMS droplets isotherms are "affinity increase" type (Shaw, 1992; Dabrowsky, 2001). This adsorption behavior confers extensive interfacial penetration and is further confirmed by SEM (Fig. 4). Densely packed adsorbed nanoparticle layers with interfacial aggregation are observed over a wide range of solution conditions. Both liquid and cross-linked PDMS droplets show strongly pH-dependent adsorption of hydrophobic nanoparticles in agreement with DLVO theory, but in contrast to hydrophilic silica nanoparticle adsorption. SEM indicated the presence of a rigid interfacial crust layer (Fig. 4) at salt concentrations corresponding to interfacial saturation and a multi-layered interfacial particle wall at salt concentrations $\geq$ ccc. A more detailed investigation of the influence of contact angle on the adsorption of chemically hydrophobised silica nanoparticles (Simovic and Prestidge, 2004) confirmed adsorption at the droplet interface with high affinity and to interfacial coverage values equivalent to close packed multi-layers. Nanoparticle adsorption isotherms are independent of the contact angle in the range 25° to >90°, suggesting that hydrophobic attraction overcomes electrostatic repulsion in all cases for chemically modified silica and is in contrast to unmodified (hydrophilic) silica nanoparticles.

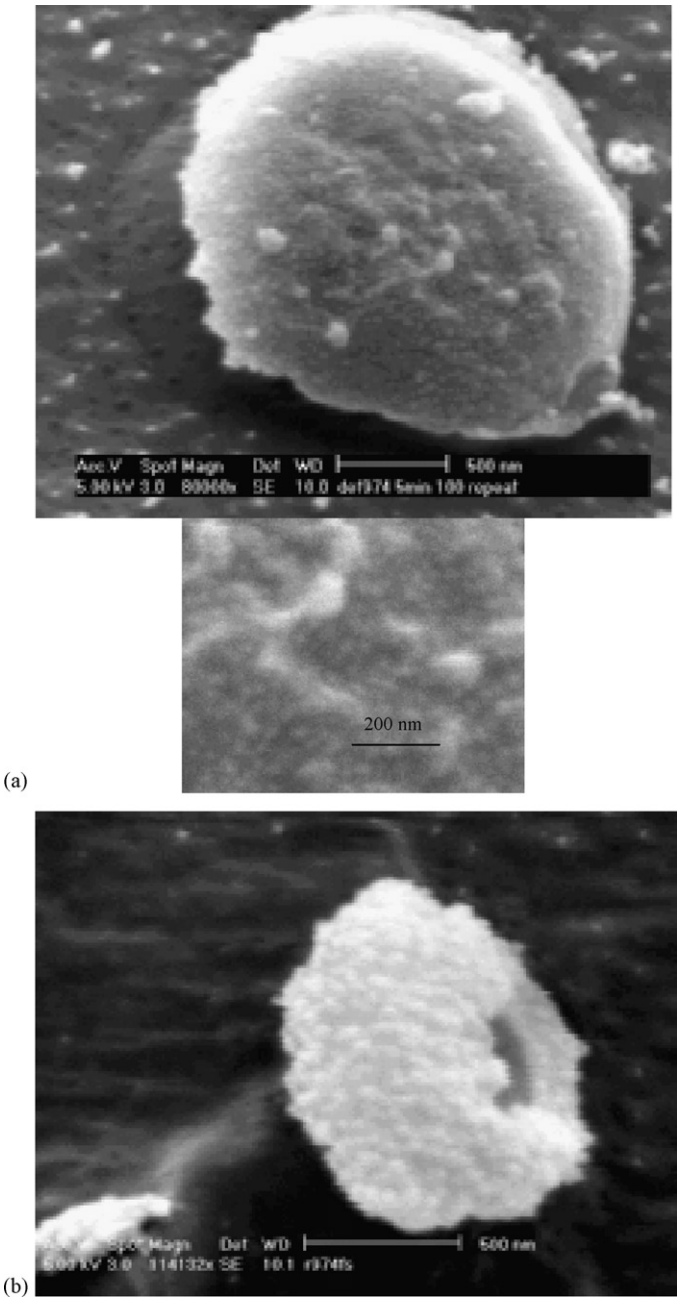

Fig. 4. Freeze-fracture SEM images of PDMS droplets coated by hydrophobic silica nanoparticles at pH 9: (a) 10^{-4} M NaCl, bottom image is a higher magnification image of the interface and (b) 10^{-1} M NaCl.

3.2. Droplet stability

Hydrophilic nanoparticle layers enhance the colloid stability of emulsion droplets, but only weakly influence the coalescence kinetics (Table 2). That is, a barrier to coalescence of only ~1 kT is introduced and kinetically unstable networks are formed at high salt concentrations. Even in the presence of a near closely packed nanoparticle layer, droplets are not resistant to coalescence by excess salt. Fig. 5 represents the size enlargement of droplets according to the Smoluchowski model for particle/droplet aggregation (Shaw, 1992). Accordingly, the rate of formation of aggregates is determined by the diffusion of the drops through the continuous phase and is a second-order process. The size enlargement process can be

Table 2
Parameters calculated from Van den Tempel and Smoluchowski models for bare and coated (by hydrophilic silica nanoparticles) PDMS droplets

	Bare droplets	Half-monolayer coated droplets	Monolayer coated droplets
k_c (min^{-1})[a]	0.15	0.009	0.0016
k_a ($\mu m^3\ min^{-1}$)[b]	350	209	42
E_{coal} (kT)[c]	0.3	1.8	6.6

[a] Coalescence rate constant (calculated from Van den Tempel model).
[b] Aggregation constant (calculated from Smoluchowski model).
[c] Energy barrier for coalescence (calculated from Smoluchowski model).

described by

$$d_t = \left(d_0^3 + \left(\frac{6k_a\phi}{\pi}\right)t\right)^{1/3} \quad (2)$$

where d_0 is the initial droplet diameter at $t = 0$, d_t the diameter at time t, k_a the second-order rate constant for aggregation and ϕ is the emulsion volume fraction. Therefore, by plotting d_t^3 versus time, we can calculate the rate constant for aggregation.

Even though Smoluchowski's treatment neglects surface forces and hydrodynamic interactions, the flocculation process in the presence of these interactions remains a second-order process and it is only the value of the rate constant that is altered. Thus, this approach can be used for assessment of the energy barriers for aggregation and has been widely used for analysing the aggregation of emulsion droplets.

Van den Tempel (described in Shaw (1992)) extended Smoluchowski's theory to include the kinetics of coalescence. The rate of coalescence was assumed to be proportional to the number of inter-droplet films and to the first-order coalescence rate constant k_c and $1/k_c$ is the life-time of the liquid film between the dispersed droplets. If coalescence is the rate controlling step, it can be shown that:

$$\left(\frac{d_0}{d}\right)^3 = \exp(-k_c t) \quad (3)$$

Therefore, k_c can therefore be calculated from the slope of a plot of $\ln(d_0/d)^3$ versus time.

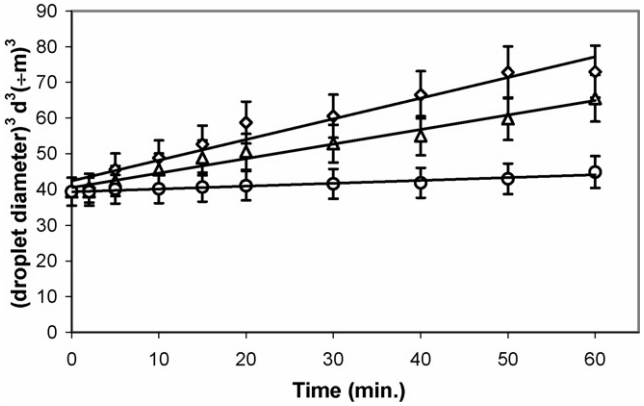

Fig. 5. Coalescence kinetics of PDMS droplets plotted in line with the Smoluchowski model (i.e. (droplet diameter)^3 vs. time): (◊) bare droplets; (△) covered by half-monolayer of hydrophilic silica; (◯) covered by monolayer of the most hydrophobic silica.

The coalescence constant calculated from the Smoluchowski model for bare droplets is close to the fast aggregation constant ($383\ \mu m^3\ min^{-1}$) and the energy barrier is less than 1 kT, which is expected in the absence of steric barrier. In the presence of a hydrophilic silica monolayer the coalescence rate constant is significantly lower and the energy barrier increases to 6.6 kT, hence the coalescence rate is retarded. However, the energy barrier is not high enough to provide substantial long-term stability.

The theory for Ostwald ripening, initially formulated by Lifshitz, Slezov and Wagner (cited in: Taylor, 1998) predicts that the cube of critical droplet radius should increase linearly with time. Ashby and Binks (2000) have reported Oswald ripening in Pickering emulsions. The mayor driving forces for Oswald ripening are the oil solubility, droplet polydispersity and presence of surfactants (Taylor, 1998). Ostwald ripening is not considered likely for the PDMS system under investigation because of the highly monodipersed droplets, low water solubility of PDMS and absence of surfactants. Furthermore, droplet size enlargement was monitored directly using optical microscopy and droplet contact/merging were evident, i.e. aggregation and coalescence are the major mechanisms for droplet size enlargement.

The highly structured and rigid adsorbed layers of hydrophobically modified silica nanoparticles significantly reduce droplet coalescence kinetics. At or above monolayer surface coverage, stable flocculated networks of droplets form and regardless of their wettability, particles are not detached from the interface during coalescence**.** Particles might undergo lateral displacements along the interface, rather than removal into the phase of preferable wettability during the coalescence process (Tambe and Sharma, 1993). At sub-monolayer nanoparticle coverages, limited coalescence is observed and interfacial saturation restricts the droplet size increase. When the nanoparticle interfacial coverage is between 70% and 100%, mesophase-like microstructures have been noted, the physical form and stability of which depends on the nanoparticle contact angle.

3.3. Release of dibutylphtalate from droplets and influence of nanoparticle coatings

DBP is poorly water-soluble and for concentrations below the solubility limit in water (~1 mg/100 ml) its release from within uncoated PDMS droplets is rapid and complete. Hydrophilic and hydrophobic silica nanoparticle coatings prepared at low salt concentration do not significantly influence DBP release (Fig. 6). At $\geq 10^{-3}$ M NaCl hydrophobic silica nanoparticles creates a rigid interfacial layer that significantly retards the DBL release rate. The release rate is further retarded in the presence of a thick interfacial particle wall prepared at 10^{-1} M NaCl (Fig. 4). Thus, depending on the salt concentration, hydrophobic silica coatings may be permeable or semipermeable. Interfacial transport is the rate limiting step in release from these coated droplets, and second-order release rate constants are in the range 0.3 and 0.05 $nm^2\ s^{-1}$; these are significantly lower than equivalent drug release rate constants from Pluronic® stabilised emulsions (4.5–45 $nm^2\ s^{-1}$) (Washington and Evans, 1995). The activation energy for crossing the interfacial barrier (from Arrhenius

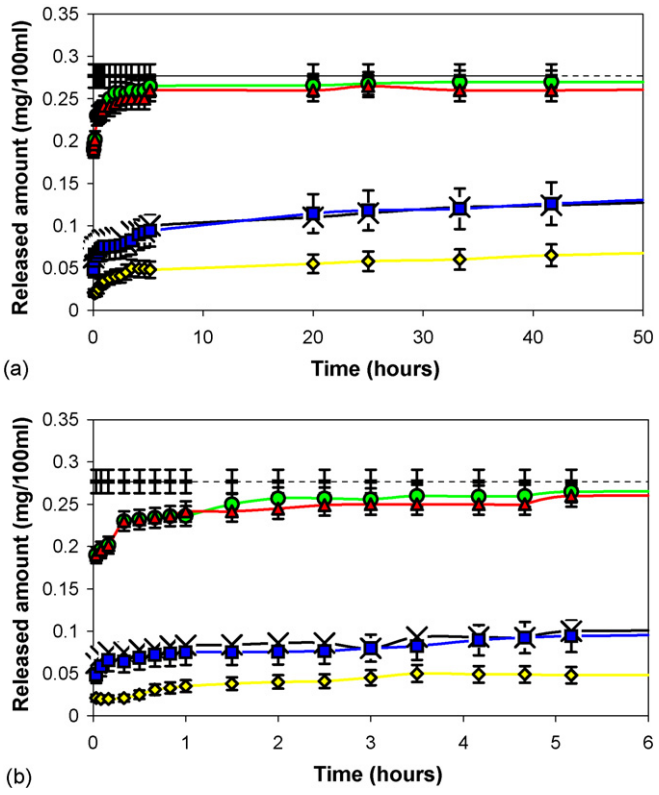

Fig. 6. Drug release profiles from liquid PDMS emulsions $\phi = 0.01$; 0.025 wt.% DBP during (a) 30 h and (b) 6 h. (◯) green, bare droplets and coated by hydrophobic silica; (△) red, 10^{-4} M NaCl; (□) blue, 10^{-3} M NaCl; (×) black, 10^{-2} M NaCl; (△) yellow, 10^{-1} M NaCl; dashed lines represents the theoretical maximum DBP concentration in the dissolution medium. N.B. the droplet surface area is not significantly altered upon nanoparticle coating nor diluting in the dissolution media. (For interpretation of the references to colour in this figure legend, the reader is referred to the web version of the article.)

plots) are ~600 kJ mol^{-1} and are significantly higher than for the Pluronic® barriers (50 kJ mol^{-1}) (Washington and Evans, 1995).

Drug release from spherical devices under sink conditions can be discussed using two limiting models (Robinson and Lee, 1978; Washington and Evans, 1995). These consider the situations where the rate of release is limited by either diffusion through the oil droplet or by an interfacial barrier. When no interfacial barrier is present, the release of drug at long times is well approximated by

$$\frac{M_t}{M_0} = 1 - \frac{6}{\pi^2}\exp(-\pi^2\tau) \tag{4}$$

M_t is the amount of drug in the particle at time t, M_0 is the initial amount of drug and dimensionless time τ is given by

$$\tau = \frac{Dt}{r^2} \tag{5}$$

D is the diffusion coefficient of the drug in the oil droplet and r is the droplet radius.

This expression can be rearranged into the linear form

$$\ln\left(1 - \frac{M_t}{M_0}\right) = \ln\left(\frac{6}{\pi^2}\right) - \frac{\pi^2 Dt}{r^2} \tag{6}$$

Thus a plot of $\ln(1 - M_t/M_0)$ against time will have a limiting slope at longer times of $-\pi^2 D/r^2$, enabling the diffusion coefficient of the drug in the oil droplet to be calculated.

When transport across the droplet interface is rate limiting, the long-time approximation for the released drug is given by

$$M_t = \frac{1}{3}Ac_0 r(1 - \exp(-3\kappa\tau)) \tag{7}$$

where A is the surface area of the sphere, c_0 the initial concentration of drug in the oil droplet and κ is given by k_1/D, where k_1 is the interfacial rate constant. Since the initial amount of drug in the droplet is $Ac_0 r/3$, this expression simplifies to

$$\frac{M_t}{M_0} = 1 - \exp\left(\frac{-3k_1 t}{r^2}\right) \tag{8}$$

Therefore, using the same linear transform as for the diffusion-limited case we obtain

$$\ln\left(1 - \frac{M_t}{M_0}\right) = \frac{-3k_1 t}{r^2} \tag{9}$$

Thus a plot of $\ln(1 - M_t/M_0)$ against time will have a limiting slope at longer times of $-3k_1/r^2$ hand hence enabling determination of the interfacial transport rate constant of the drug between the oil droplet and the release medium.

The release kinetics of the electrolytes CsCl and NaCl from an inner water phase to an outer water phase in multiple w/o/w emulsions stabilised entirely by silica nanoparticles was theoretically and experimentally described by Binks (2002) and Barthel et al. (2003). The release kinetics follows first-order kinetics and the measured rate constant (0.001 min^{-1}) was 200 times lower than that theoretically calculated (0.2 min^{-1}) based that the release rate is controlled solely by diffusion from inner water phase through oil phase into the outer water phase.

It is also feasible to assimilate nanoparticle coated liquid PDMS droplets to microcapsules in which the internal drug concentration decreases with time. In that case the drug release kinetics can be represented by an exponential relationship (Robinson and Lee, 1978; Rollet and Bardon, 2000):

$$\ln(Q_0 - Q) = \ln Q_0 - kt \tag{10}$$

where Q_0 is the initial amount of drug present in the droplets, Q the amount released at time t and k is the first-order kinetic constant (min^{-1}). The kinetic release rate constant was calculated to be 0.0003 min^{-1} (for hydrophobic nanoparticle coatings prepared at 10^{-3} and 10^{-2} M NaCl) and 0.0001 min^{-1} (prepared at 10^{-1} M NaCl). In comparison with reported data for kinetic release rate constants for microcapsules (Rollet and Bardon, 2000) and multiple emulsions (Binks, 2002) these values are approx. 1000 and 10 times lower, respectively. These comparisons confirm that the sustained release effect is significant for the nanoparticle coated PDMS droplet system under investigation here.

A schematic representation of the interplay between nanoparticle type, solution properties, interfacial structure and release characteristics is given in Fig. 7.

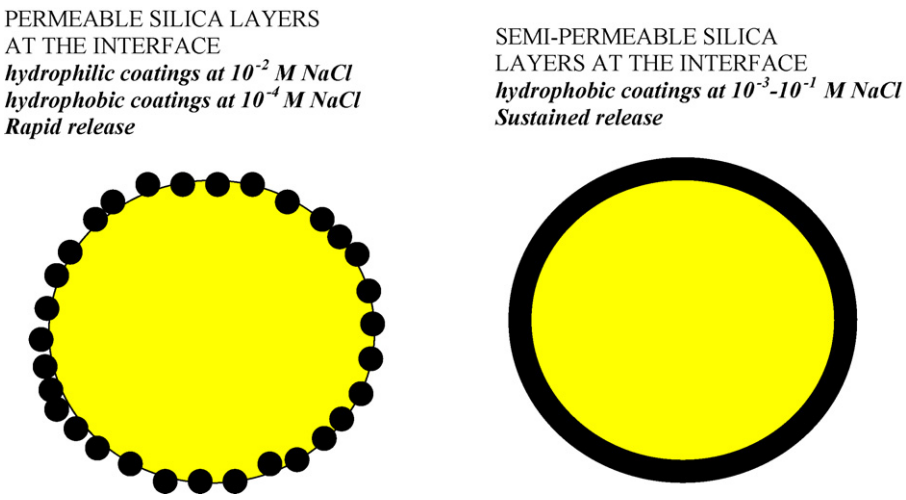

Fig. 7. Schematic representation of interplay between nanoparticle type, solution properties, interfacial structure of PDMS droplets and the release characteristics.

4. Conclusions

Nanoparticle adsorption thermodynamics, the adsorbed layer structure and the release behavior are interrelated and controlled by the nanoparticle hydrophobicity and salt concentration employed in the encapsulation process. Encapsulating nanoparticle layers at the emulsion droplet interface may be engineered to improve droplet stability and control the release kinetics of model lipophilic molecules. Significant sustained release effects can be achieved using hydrophobic silica nanoparticles.

Acknowledgements

The Australian Research Council's Special Research Centre for Particle and Material Interfaces is acknowledged for supporting this research. Dr. Peter Self is thanked for assistance with the SEM investigations and analysis.

References

Adamzcyk, Z., Weronski, P., 1999. Application of DLVO theory for particle deposition problems. Adv. Colloid Interf. Sci. 83, 137–226.

Adamzcik, Z., 1989. Particle deposition from flowing suspensions. Colloid Surf. A 39, 1–37.

Ashby, N.P., Binks, B.P., 2000. Pickering emulsions stabilised by laponite clay particles. Phys. Chem. Chem. Phys. 2, 5640–5646.

Aveyard, R., Binks, B.P., Clint, J.H., 2003. Emulsions stabilised solely by colloidal particles. Adv. Colloid Interf. Sci. 100–102, 503–546.

Barthel, H., Binks, B.P., Dyab, A., Fletcher, P., 2003. Multiple emulsions. Patent US2003/0175317.

Binks, B.P., Lumsdon, S.O., 1999. Stability of oil-in-water emulsions stabilised by silica particles. Phys. Chem. Chem. Phys. 1, 3007–3016.

Binks, B.P., Kirkland, M., 2002. Interfacial structure of solid-stabilised emulsions studied by scanning electron microscopy. Phys. Chem. Chem. Phys. 4, 3727–3733.

Binks, B.P., Lumsdon, S.O., 2000a. Catastrophic phase inversion of water-in-oil emulsions stabilised by hydrophobic silica. Langmuir 16, 2539–2547.

Binks, B.P., Lumsdon, S.O., 2000b. Transitional phase inversion of solid-stabilised emulsions using particle mixtures. Langmuir 16, 3748–3756.

Binks, B.P., Lumsdon, S.O., 2000c. Influence of particle wettability on the type and stability of surfactant-free emulsions. Langmuir 16, 8622–8631.

Binks, P.B., 2002. Multiple emulsions stabilised solely by nanoparticles, Proceedings of Third World Congress on Emulsions. Lyon, CME, Paris, pp. 1–10.

Binks, B.P., Clint, J.H., Mackenzie, G., Simcock, C., Whitby, C.P., 2005. Naturally occuring spore particles at planar fluid interfaces and in emulsions. Langmuir 20, 2069–2074.

Blanko-Prieto, M.J., Fattal, E., Puisieux, F., Courvreur, P., 1998. The multiple emulsion as a common step for the design of polymeric microparticles. In: Multiple Emulsions: Structure, Properties Application. Editions De Sante.

Bleier, A., Matijevic, E., 1997. Heterocoagulation. Part 3. Interaction of polyvinyl chloride latex with Ludox HS silica. J. Chem. Soc., Faraday Trans. 62, 1347–1359.

Chambin, O., Bellone, C., Champion, D., Rochat-Gonthier, M.H., 2000. Dry adsorbed emulsion. 1. Characterisation of anintricate physico-chemical structure. J. Pharm. Sci. 89, 991–999.

Chambin, O., Bérard, V., Rochat-Gonthier, M.H., Pourcelot, Y., 2002. Dry adsorbed emulsion. 2. Dissolution behaviour of an intricate formulation. Int. J. Pharm. 235, 169–178.

Courveur, P., Dubernet, C., Puisieux, F., 1995. Controlled drug delivery with nanoparticles: current possibilities and future trends. Eur. J. Pharm. Biopharm. 41, 2–13.

Dabrowsky, A., 2001. Adsorption-from theory to practice. Adv. Colloid Interf. Sci. 93, 135–224.

Garti, N., 1997a. Double emulsions—scope, limitations and new achievements. Colloid Surf. A: Physicochem. Eng. Aspects 123/124, 233–246.

Garti, N., 1997b. Progress in stabilization and transport phenomena of double emulsions in food applications. Lebensm. Wiss. Technol. 30, 222–235.

Goller, M.I., Obey, T.M., Declan, O.H.T., Vincent, B., Wegener, M.R., 1997. Inorganic "silicone oil" microgels. Colloid Surf. A 123, 183–193.

Hogg, R., Healy, T.W., Fuerstenau, D.W., 1966. Mutual coagulation of colloidal dispersions. J. Chem. Soc., Faraday Trans. 62, 1638–1650.

Horozov, T.S., Binks, B.P., 2006. Particle-stabilized emulsions: a bilayer or a bridging monolayer? Angew. Chem. Int. Ed. 45, 773–776.

Hunter, R.J., 1993. Introduction to Modern Colloid Science. Oxford Science Publications.

Mehnert, W., Mader, K., 2001. Solid lipid nanoparticles: production, characterization and applications. Adv. Drug Deliv. Rev. 47, 165–196.

Müller, R.H., Mäder, K., Gohla, S., 2000. Solid lipid nanoparticles (SLN) for controlled drug delivery—a review of the state of the art. Eur. J. Pharm. Biopharm. 50, 161–177.

Müller, R.H., Radtke, M., Wissing, S.A., 2002. Solid lipid nanoparticles (SLN) and nanostructured lipid carriers (NLC) in cosmetic and dermatological preparations. Adv. Drug Deliv. Rev. 54, S131–S155.

Obey, T.M., Vincent, B., 1994. Novel monodisperse "silicone oil"/water emulsions. J. Colloid Interf. Sci. 163, 454–463.

O'Donnell, P.B., McGinity, J.W., 1997. Preparation of microspheres by the solvent evaporation technique. Adv. Drug Deliv. Rev. 28, 25–42.

Oza, K.P., Frank, S.G., 1989a. Multiple emulsions stabilized by colloidal microcrystalline cellulose. J. Disper. Sci. Technol. 10, 163–185.

Oza, K.P., Frank, S.G., 1989b. Drug release from emulsions stabilized by colloidal microcrystalline cellulose. J. Disper. Sci. Technol. 10, 187–210.

Prestidge, C.A., Barnes, T., Simovic, S., 2004. Polymer and particle adsorption at the PDMS droplet–water interface. Adv. Colloid Interf. Sci. 108/109, 105–118.

Robbe-Tomine, L., Hen-Ferrenbach, C., 1998. Multiple Emulsions: Structure, Properties and Applications. Editions De Sante, Paris, pp. 141.

Robinson, R., Lee, J., 1978. The physical approach: oral and parentheral. In: Sustained and Controlled Release Drug Delivery Systems. Marcel Dekker Inc., NewYork, pp. 124–210.

Rollet, M., Bardon, J., 2000. Dry adsorbed emulsions. In: Pharmaceutical Emulsions and Suspensions. Marcel Dekker Inc., New York, pp. 361–381.

Sawyer, L., Grubb, D., 1987. Polymer Microscopy. Chapman and Hall, London, p. 76.

Shaw, D.J., 1992. Introduction to Colloid and Surface Chemistry. Butterworth, Oxford, p. 128.

Simovic, S., Prestidge, C.A., 2003a. Hydrophilic silica nanoparticles at the PDMS droplet–water interface. Langmuir 19, 3785–3792.

Simovic, S., Prestidge, C.A., 2003b. Adsorption of hydrophobic silica nanoparticles at the PDMS droplet–water interface. Langmuir 19, 8364–8370.

Simovic, S., Prestidge, C.A., 2004. Nanoparticles of varying hydrophobicity at the emulsion droplet–water interface: adsorption and coalescence stability. Langmuir 20, 8357–8365.

Tadros, Th.F., Vincent, B., 1983. Encyclopedia of Emulsion Technology, Basic Theory, vol. 1. Marcel Dekker Inc.

Tambe, D.E., Sharma, M.M., 1993. Factors controlling the stability of colloid-stabilized emulsions. I. An experimental investigation. J. Colloid Interf. Sci. 15, 244–254.

Tambe, D.E., Sharma, M.M., 1994. The effect of colloidal particles on fluid–fluid interfacial properties and emulsion stability. J. Colloid Interf. Sci. 52, 1–63.

Taylor, P., 1998. Ostwald ripening in emulsions. Adv. Colloid Interf. Sci. 75, 107–163.

Vignati, E., Piazza, R., Lockhart, T.P., 2003. Pickering emulsions: interfacial tension, colloidal layer morphology, and trapped-particle motion. Langmuir 19, 6650–6656.

Washington, C., Evans, K., 1995. Release rate measurements of model hydrophobic solutes from submicron triglyceride emulsions. J. Control. Release 33, 383–390.

Yan, N., Gray, M.R., Masliyah, J.H., 2001. On water-in-oil emulsions stabilized by fine solids. Colloid Surf. A: Physicochem. Eng. Aspects 193, 97–107.

Yan, N., Maham, Y., Masliyah, J.H., Gray, M.R., Mather, A.E., 2000. Measurement of contact angles for fumed silica nanospheres using enthalpy of immersion data. J. Colloid Interf. Sci. 228, 1–6.